*Clays and Clay Minerals*, Vol. 48, No. 2, 204–212, 2000.

# CHARACTERISTICS OF CLAY MINERALS IN GOUGES OF THE DONGRAE FAULT, SOUTHEASTERN KOREA, AND IMPLICATIONS FOR FAULT ACTIVITY

CHANG OH CHOO[1] AND TAE WOO CHANG[2]

[1] Environmental Geology Division, Korea Institute of Geology, Mining and Materials, Taejon, 305-350, Korea
[2] Department of Geology, Kyungpook National University, Taegu, 702-701, Korea

**Abstract**—The Dongrae fault within the Yangsan fault system is considered one of the major faults in the southeastern part of Korea, extending over 150 km. The results of K-Ar radiogenic dating of fault gouges collected from six localities show a relatively wide range in age from 57.5 million years ago (Ma) to 40.3 Ma. Fault gouges are composed of newly formed minerals, including smectite, illite, zeolite, kaolinite, K-rich feldspar, apatite, and pyrite. The occurrence of abundant smectite and illite-1$M_d$ with lesser quantities of zeolite suggests that the fault gouges experienced hydrothermal alteration at low temperatures. Smectite is probably unstable relative to other clay minerals, such as illite and zeolite. Considering that filiform mordenite is replacing the smectite, we suggest that mordenite formed by recrystallization involving a solid-state transformation. Under high fluid/rock ratios, smectite seems to have formed in the early stage of alteration. In contrast, zeolite minerals and authigenic K-rich feldspar progressively appeared with time as the fluid/rock ratio decreased with the changing chemistry of the hydrothermal fluids. The composition of clay minerals in the gouge materials probably was controlled by the chemistry and the amount of circulating fluids derived from adjacent granitic rocks.

**Key Words**—Dongrae Fault, Gouge, Illite, K-Ar Radiogenic Dating, Smectite, Zeolite.

## INTRODUCTION

There have been many studies on fault gouges since 1980, mainly focused on the formation processes of gouges (Chester *et al.,* 1993), mechanical properties and permeability of gouges (Morrow *et al.,* 1984; Caine *et al.,* 1996), composite planar fabric developed on gouge zones (Chester and Logan, 1987; Takagi and Kobayashi, 1996), and K-Ar dating to obtain the time of the movement of the major fault (Kralik *et al.,* 1987; Shibata and Tagaki, 1988; Tagaki *et al.,* 1989; Tanaka *et al.,* 1995). Lyons and Snellenburg (1971) were the first to determine the absolute age of last motion along the faults by using K-Ar techniques on the authigenic illitic fraction in fault gouges.

The Yangsan fault system is the largest in southeastern Korea. It trends NNE-SSW and comprises a number of major faults, *i.e.,* the Yangsan, Dongrae, Eonyang, Moryang, Ilkwang, and Ulsan faults, most of which extend over 150 km (Figure 1). Although the level of seismicity in Korea is low compared to northeastern China and Japan, some great earthquakes have occurred during historic time with considerable destruction. From A.D. 2 to 1989, at least 126 earthquakes have occurred along the Yangsan fault system (Lee and Jin, 1991). These earthquakes mostly occurred in the Kyungju-Ulsan areas, located within the fault system. During the 1990's, the frequency and magnitude of earthquakes along the Yangsan fault system were more significant than previously. For instance, since 1997, there have been more than 50 weak earthquakes in the vicinity of, or along, the Yangsan fault system.

Several nuclear power plants were constructed in the vicinity of the Yangsan fault system during the last two decades. Because the Yangsan fault system is considered an active fault in Korea, it has been extensively studied. However, although there are limited geophysical data (Kim and Kim, 1983; Lee and Na, 1983; Kim and Lee, 1988; Lee *et al.,* 1992), the history of the fault system still cannot be reconstructed. Moreover, no mineralogical study on the fault gouges in the Yangsan fault system has been undertaken, despite the potential of such studies to understand the evolution of the fault system. The purpose of this study is to understand the origin of the gouge materials in the Dongrae fault, one of the major faults in the Yangsan fault system, and to estimate the age of fault activity using K-Ar dates of the K-bearing minerals.

## GEOLOGICAL SETTING OF THE DONGRAE FAULT

The Dongrae fault occurs in the Kyeongsang sedimentary basin. The basin is situated in the southeastern part of the Korean peninsula and comprises sedimentary rocks and subordinated igneous rocks, with ages ranging from Cretaceous to early Tertiary. Despite the intensive volcanism and plutonism occurring in the basin, deformation is negligible except for normal and strike-slip faulting (Kim, 1987). Strike-slip faults trend mostly N-S to NE-SW in the southeastern marginal area of the basin. The area of the present study is between longitude 129°00′–129°25′ and latitude 35°12′–35°40′ and located eastward of the Yangsan fault. We investigated the Eungsang-Gokcheonri

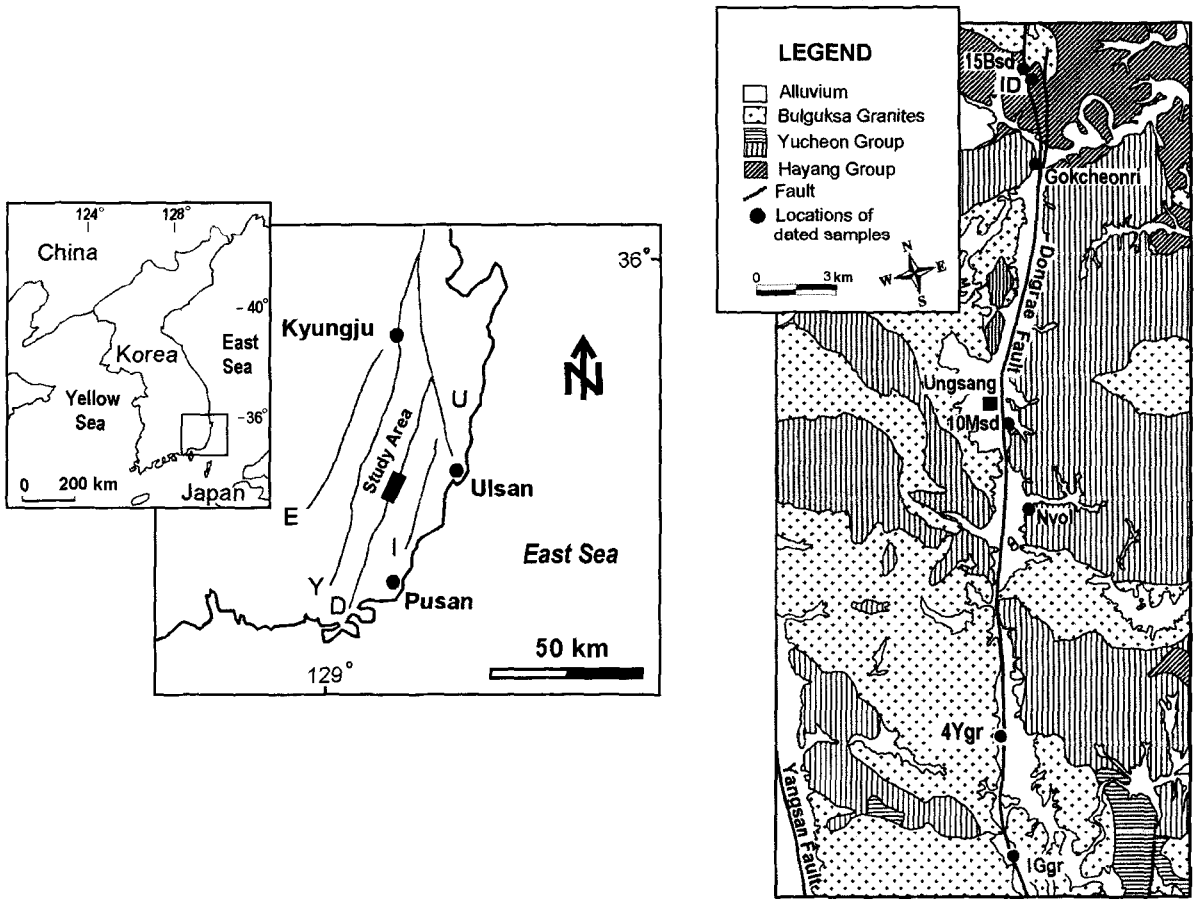


Figure 1. Yangsan Fault System in the southeastern part of Korea and geological map of the study area in the Dongrae fault. Symbols: D: Dongrae fault, E: Eonyang fault, I: Ilkwang fault, U: Ulsan fault, and Y: Yangsan fault.

areas along a linear valley developed by the Dongrae fault. This area is underlain by the Hayang group, the Yucheon group, and the Bulguksa granites (Figure 1). All these strata are Cretaceous to early Tertiary in age.

The Hayang group is composed of shales and sandstones, both of which show well-developed laminations and bedding planes. In the northern part of the study area, the Hayang group is hydrothermally altered by the Bulguksa granites, which have produced intense hornfels. The bedding planes generally strike E–W and dip 10–20°S, but the sedimentary rocks are heavily disturbed near the fault.

The Yucheon group, 2000–3000 m thick, consists of volcanic rocks and associated sedimentary rocks. The group is characterized by the dominance of volcanic rocks. The volcanic sequence of this group can be divided into andesitic rocks in the lower part and rhyolitic rocks in the upper part. Andesitic rocks are composed of andesite, trachytic andesite, pyroxene andesite, lapilli tuff, and volcanic breccia. Rhyolitic rocks are composed of spherulitic rhyolite, rhyolitic or rhyodacitic-welded tuff, and rhyolite porphyry. A few weak hydrothermal-alteration zones exist on the both sides of the Dongrae fault, which are related to the effects of granite intrusion.

The Bulguksa granites, ranging in age from Cretaceous to late Tertiary, consist of granodiorite, biotite granite, hornblende granite, and aplitic granite. Some of these granites intruded the Hayang and Yucheon groups and commonly show thermal alteration. In particular, aplite occurs in the southern part of the study area as a late stage intrusive into biotite granite. The late Cretaceous granitic rocks in this area are calc-alkaline, I-type, and magnetite-series intrusives that occur in the subduction zone (Shimazaki and Lee, 1981).

The Dongrae fault is not a simple single fault. The fault is complex with many small faults and fracture zones containing gouge materials. Fault zones in the Dongrae fault are subdivided into a fault core in the central part and a damage zone at the margins. A fault core consists of thin gouge and narrow cataclastic zones bounded by a much thicker damage zone. The intensity of deformation and alteration drastically in-

https://doi.org/10.1346/CCMN.2000.0480206 Published online by Cambridge University Press

Table 1. X-ray diffraction data and K-Ar ages of fault gouges.

| Sample | Host rock | Gouge color | Minerals[1] | $K_2O$ (wt. %) | $^{40}Ar^*$ (%)[2] | $^{40}Ar^*$ ($10^{-6}$ cm$^3$/g) | Age (Ma) |
|---|---|---|---|---|---|---|---|
| 10Msd | Sedimentary rock | gray | ill ≫ qtz > py | 6.82 | 75.8 | 27.62 | 57.5 ± 1.4 |
| 15Bsd | Sedimentary rock | brown | sm ≫ zeol > qtz, ill | 0.91 | 19.5 | 2.55 | 40.3 ± 1.4 |
| 1Ggr | Granite | dark brown | sm ≫ qtz > zeol > ill | 1.66 | 48.5 | 6.01 | 51.4 ± 1.3 |
| 4Ygr | Granite | whitish gray | sm > ill | 1.42 | 45.3 | 5.50 | 54.9 ± 1.4 |
| Nvol | Andesitic rock | gray | qtz ≫ ill, kaol | 5.65 | 80.3 | 17.27 | 43.6 ± 1.1 |
| ID | Acidic dike | dark green | feld, ch | 0.99 | 33.4 | 3.15 | 45.6 ± 1.5 |
| Gokcheonri | Sedimentary rock | gray | sm ≫ zeol > Ksp | n.d.[3] | n.d. | n.d. | n.d. |

[1] ch: chlorite; feld: feldspars; ill: illite; kaol: kaolinite; Ksp: K-rich feldspar; py = pyrite; qtz: quartz; sm: smectite; zeol: zeolite.
[2] Ar: radiogenic argon.
[3] n.d.: not determined.

creases from the damage zone through the cataclastic zone to the gouge zone. The types of gouge material contained in the fault zone depend on the locality. For instance, the host rocks of the fault gouge near the Cheongryang area of Ulsan City are dark green sandstone and gray siltstone that were thermally metamorphosed by the intrusion of the Bulguksa granites. The fault core in this area is >40 m in width. In addition, two sets of fault gouges occur at 2-m intervals. Each gouge zone is 3–6 cm in width and is parallel. In the Gokcheonri area, the fault zone is gray in color and 5 m in width.

## EXPERIMENTAL METHODS

Fault gouges were collected at six localities (Figure 1) along the Dongrae fault in the study area. Gouge samples were preserved in plastic bags to maintain original water content. Clay minerals of gouge materials are amenable to isotope analyses, but only those clays formed at the time of the fault movement will give a reliable age of the event. Diagenetic minerals or those that form during cataclastic deformation must be excluded. Therefore, diagenetic minerals, which tend to form larger grain sizes, were separated from the clay-size minerals of the fault gouges by applying ultrasonic-separation techniques.

The bulk and clay fraction of the samples were determined by X-ray diffraction (XRD) analysis using a Rigaku Model RAD-3C diffractometer with Ni-filtered CuKα radiation in the range of 3–65 °2θ. The clay was separated by ultrasonic disaggregation, gravity settling, and centrifugation. Oriented clay-mineral aggregates were prepared on glass slides after <1-μm suspensions were collected. Samples containing smectite were examined in the 3–35 °2θ range for both preferred-oriented aggregate samples and random-powder samples, with step scanning at intervals of 0.02 °2θ for 3 s each. To differentiate between illite, smectite, and interstratified illite-smectite (I-S) minerals, XRD data were obtained from air-dried and glycolated samples.

Because gouge materials are fragile, petrographic thin sections were carefully prepared after the gouge fractions were embedded in low-viscosity resin. Quantitative chemical analyses on polished thin sections were made by a Cameca Camebax SX50 microprobe operating at an acceleration voltage of 15 kV, a beam current of 15 nA, and a spot size of 10 μm. Back scattered electron (BSE) images were made of the polished thin sections in the Cameca instrument. Textures of bulk gouges were observed with a JEOL JSM 840A scanning electron microscope (SEM) and chemical analyses were made using energy-dispersive spectrometry (EDS). Only gouges free of detrital contamination were prepared for K-Ar isotope measurements. Clay fractions containing illite or I-S minerals were used for K-Ar dating after examining by XRD.

## RESULTS

### *XRD data of gouge materials*

Most gouge samples consist predominantly of illite, smectite, and quartz, with accessory minerals such as zeolite, kaolinite, and pyrite. The XRD results are summarized in Table 1 and representative patterns are given in Figure 2. Fault gouge from site 10Msd was found to contain only illite, whereas gouges at other sites contain smectite, illite, kaolinite, and zeolites. Illite is notable by its presence in all samples examined except for the Gokcheonri gouge. An XRD peak at ~10 Å occurred both before and after glycolation, indicating that there are no detectable mixed-layer expandable components present in the illite. Illite-1$M_d$ is commonly characterized by elevated background between 20–33 °2θ and by the diminution of intensities of *hkl* reflections with $k \neq 3n$.

Smectite occurs in all areas except 10Msd and Nvol. Smectite is most abundant in the Gokcheonri area. The basal spacings of smectite are variable depending on localities and water content of the samples, but most $d(001)$ values occur at 14–15 Å at an air-dried state. After glycol treatment, the $d(001)$ peak occurs at 16.92 Å in sample 15Bsd and at 18.71 Å in the Gokcheonri sample. All smectites are dioctahedral, as indicated by the (060) reflection at 1.49–1.50 Å.

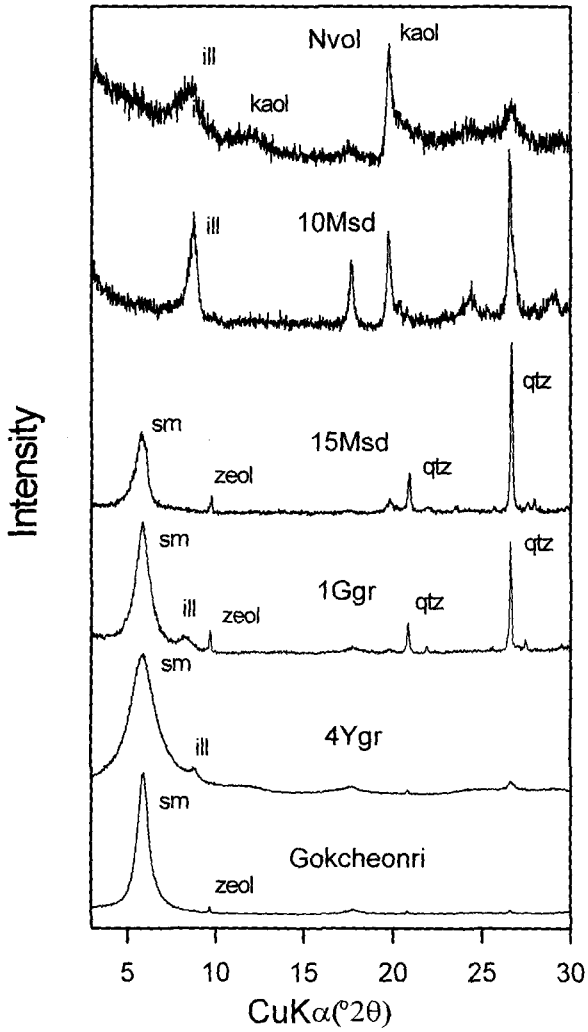


Figure 2. Representative X-ray diffractograms of clays associated with faults. Symbols: sm: smectite, ill: illite, qtz: quartz, zeol: zeolite.

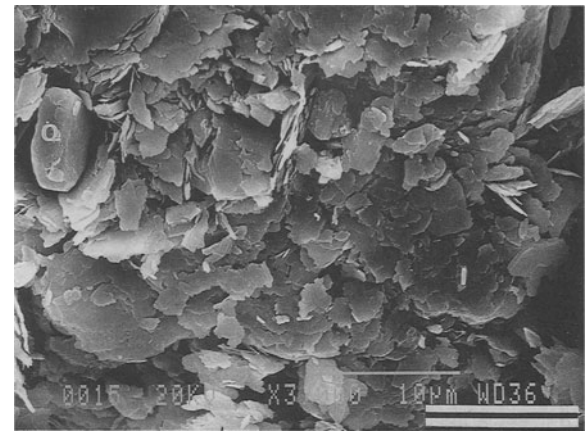


Figure 3. Scanning electron micrographs of illite in gouge from sedimentary rock (sample 10Msd). Symbols: I: illite, Q: quartz. Scale is 10 μm.

*SEM observations*

Crystallites of illite are ≤10 μm in length and show compact textures (Figure 3). Illite shows subhedral crystals and exhibits aggregates of near equal-size crystals. From XRD, these illites are $1M_d$. Illite appears to have formed in feldspar and in gouge matrix. Based on electron microprobe data, illite associated with feldspar phenocrysts shows higher K content relative to illite in the matrix; the K content is 0.75–0.78 atoms per $O_{10}(OH)_2$ for illite in phenocrysts and 0.61–0.70 atoms per $O_{10}(OH)_2$ for illite in matrix. In addition, illite in feldspar phenocrysts also has a higher K content in the interlayer sites.

Smectite is ubiquitous in several areas. In the Gokcheonri area, it is characterized by curled flakes ~2–3 μm in size and equigranular crystallites (Figure 4). EDS indicates that these samples contain Ca and trace Na, which are probably present as interlayer cations. Illite-smectite mixed-layer phases formed from feldspar contain Ca with trace K content as the interlayer cation. Thus, the precursor was probably K-bearing feldspar. Smectite in the gouge of granitic rocks occurs as curled flakes along feldspar cleavages. In some cases, smectite is closely associated with zeolite minerals.

Zeolite minerals are common, especially in sedimentary rocks such as the 15Msd and Gokcheonri gouges. In the fault gouges of the Dongrae fault, mordenite occurs in sample 15Msd, whereas heulandite is found in the Gokcheonri sample. Heulandite occurs as veins or disseminated grains in the smectite matrix, with lath-shaped crystals of 5–10 μm. Heulandite occurring in veinlets shows homogeneous chemistry. Replacement of smectite by mordenite predominantly occurs at flake edges and sometimes the entire smectite matrix is replaced (Figure 5). The width of each fiber of mordenite is <0.2 μm.

Although kaolinite is generally not detected by XRD, it is occasionally observed by SEM. Kaolinite is the dominant component after illite in the gouge sample Nvol, the volcanic host rock, with crystals of tens of micrometers in size. Kaolinite shows vermiform or "book-stacking" texture. There is no evidence that kaolinite paragenetically coexists with precursor minerals, such as feldspars or clay minerals, that may provide the required chemical components to form kaolinite.

Hydrothermal effects are indicated by accessory or trace minerals. Pyrite commonly occurs in most gouge materials, but is especially abundant in the gouge of sedimentary rocks as found in the 10Msd and Gokcheonri samples. Pyrite is disseminated as euhedral crystals in illite matrix, especially in sample 10Msd. K-rich feldspar is closely associated with heulandite veinlets (Figure 6). Apatite, <1 μm in size, occurs as

https://doi.org/10.1346/CCMN.2000.0480206 Published online by Cambridge University Press

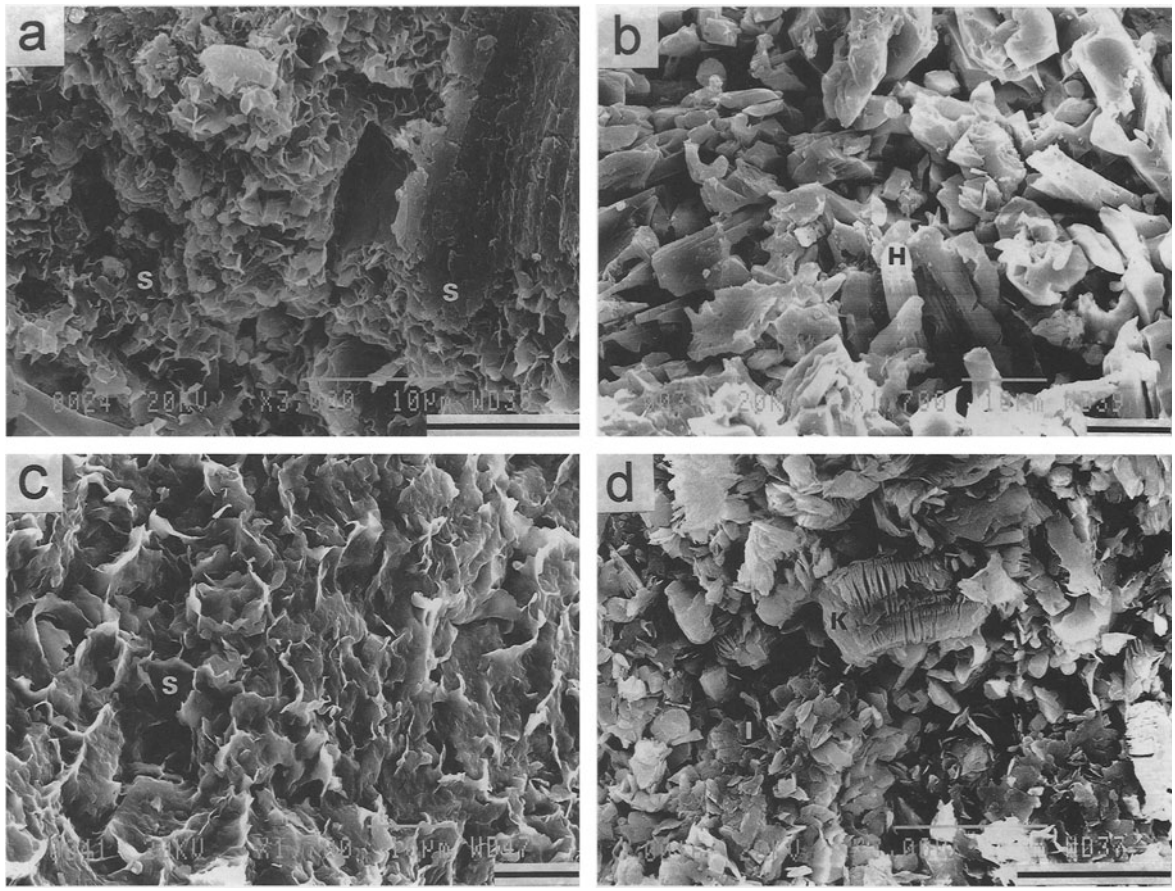


Figure 4. Scanning electron micrographs of various clays formed in gouges. a) Smectite from sedimentary rock (Gokcheonri area), b) heulandite aggregates in sedimentary rock (Gokcheonri area), c) smectite from Bulguksa granites (sample 1Ggr), and d) vermiform kaolinite in matrix of illite from volcanic rock (sample Nvol). Symbols: S: smectite, I: illite, K: kaolinite. Each scale is 10 μm.

a trace mineral in the Gokcheonri gouge, disseminated in the smectite matrix.

*The K-Ar ages of gouge materials*

The results of K-Ar dating of the gouge materials in the Dongrae fault are given in Table 1. The K-Ar dates of fault gouges show a relatively wide range from 57.5 to 40.3 million years ago (Ma). Gouges in the fault zones developed around the Bulguksa granites are not only similar in mineral assemblages and total $K_2O$ content, but also represent nearly the same ages; 51.4 Ma for 1Ggr and 54.9 Ma for 4Ygr. Similarly, Chang and Choo (1998) found that the K-Ar ages of illitic material from gouges in the Bulguksa granites near the Yangsan fault, which are located ~20 km away from the study area, range from 58.7 to 50.3 Ma.

Two gouge samples from the Hayang group composed of sedimentary rocks show quite different ages, 40.3 Ma for 15Msd and 57.5 Ma for 10Msd. Both of these gouges differ also in mineral assemblages and $K_2O$ content. Gouge (sample Nvol) derived from the volcanic rocks of the Yucheon group is enriched in $K_2O$ with an age of 43.6 Ma. The acidic dike, which is cut by a minor fault, shows a whole-rock date of 45.6 Ma.

## DISCUSSION

*Origin of alteration minerals in gouges*

Approximately 50–95% of the gouge materials are clay minerals, based on XRD and SEM data. According to thin section petrography and SEM images, illite and smectite occupy most pore space in the gouges. The intergranular shapes suggest precipitation or neoformation during hydrothermal alteration. In particular, the illite-1$M_d$ shows sharp crystal outlines and occurs as crystal aggregates composed of nearly the same size crystals (*e.g.,* sample 10Msd). These observations strongly suggest that the illite formed from dissolution/precipitation. The features relating to illite precipitation from hydrothermal fluids have been described elsewhere, for example, the Salton Sea (Yau *et al.,* 1987) and the Bobae sericite mine of Korea (Choo,

https://doi.org/10.1346/CCMN.2000.0480206 Published online by Cambridge University Press

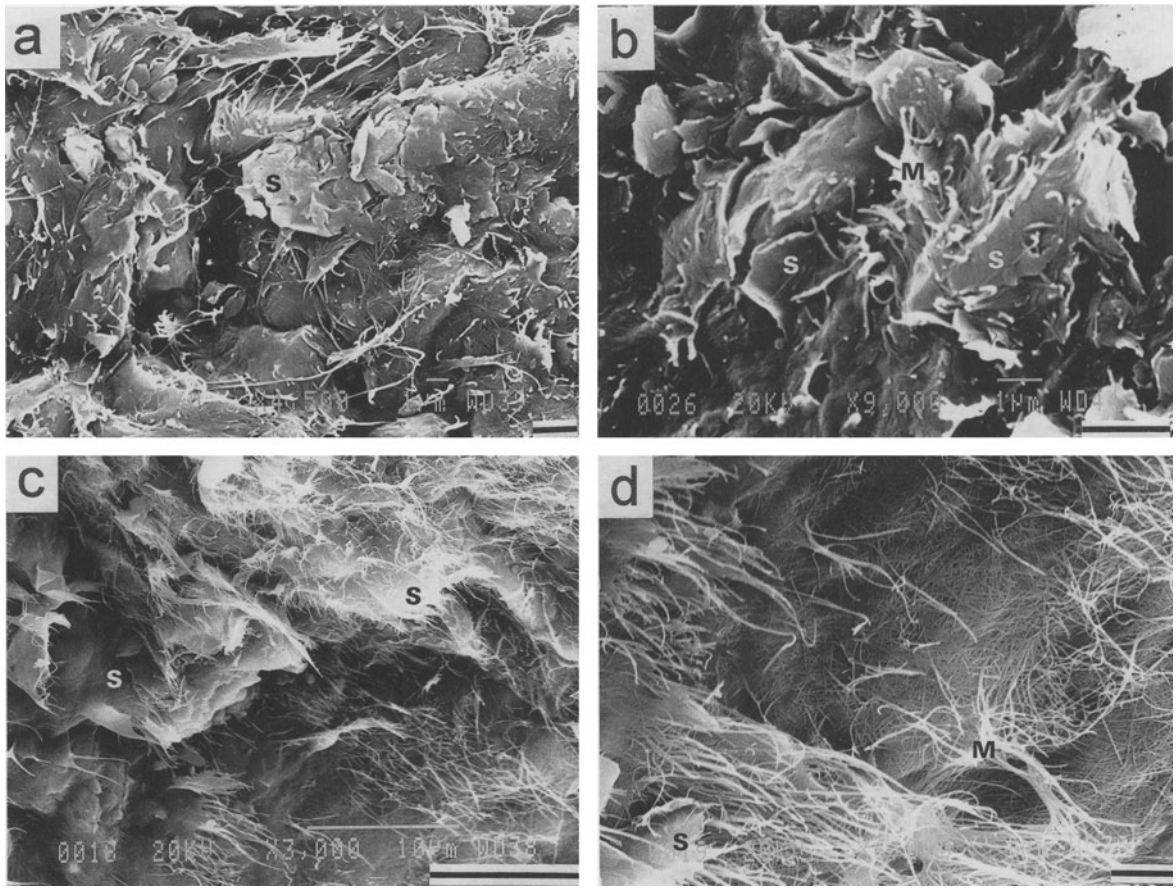


Figure 5. Scanning electron micrographs of smectite and mordenite in gouges formed in sedimentary rocks (sample 15 Msd). a) Smectite partially replaced by mordenite, b) mordenite replaces the edge of smectite, c) and d) filiform mordenite and remnants of smectite replaced. Symbols: S: smectite, M: mordenite. Scale of (a), (b), and (d) is 2 μm and scale of (c) is 10 μm.

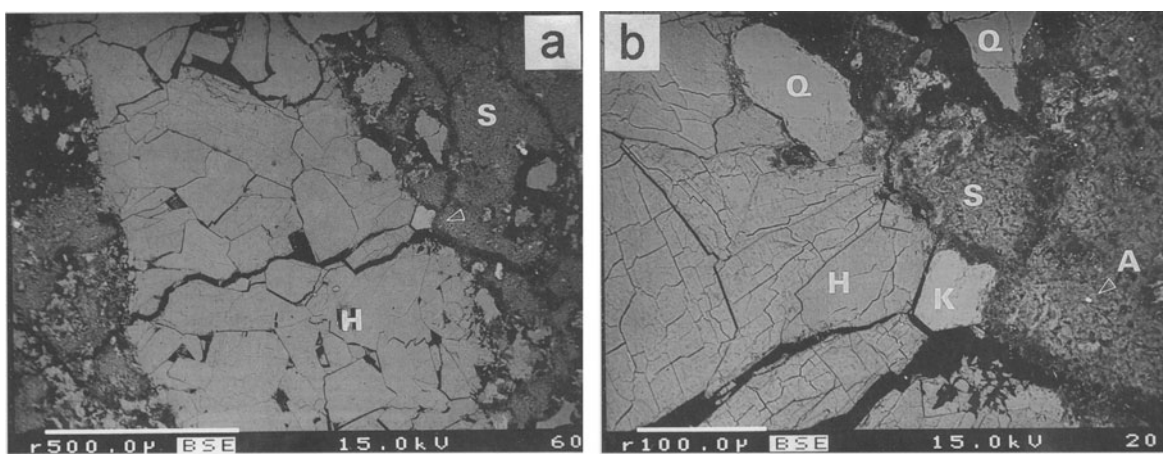


Figure 6. Back-scattered images of heulandite from the Gokcheonri area. a) Heulandite vein and smectite, b) enlarged image of area (arrow) of (a). Symbols: H: heulandite, S: smectite, Q: quartz, K: K-rich feldspar, A: apatite. Scale of (a) is 500 μm and scale of (b) is 100 μm.

https://doi.org/10.1346/CCMN.2000.0480206 Published online by Cambridge University Press

1996). Baxter Grubb *et al.* (1991) found that illite-1$M_d$ occurs initially, regardless of origin, either from direct crystallization from solution or as replacement of smectite. However, in most natural systems, morphology and the polytype of illite significantly changes with increasing degree of alteration (Inoue *et al.,* 1988; Baxter Grubb *et al.,* 1991).

Mordenite is commonly formed along with smectite during the initial stages of volcanic-glass dissolution (Kerrisk, 1983). As replacement proceeds, smectite is transformed to filiform or fibrous bundles of mordenite. There is a continuum in structure and morphology between mordenite and smectite. Therefore, mordenite formed by recrystallization of smectite by a solid-state transformation. Mordenite and heulandite appear to be stable phases in gouges because they occur as veinlets, aggregates in interstitial spaces, or replacement of precursor minerals. However, no genetic relationship between both zeolite minerals was found in the fault-gouge materials because they do not coexist in the same sample. There is a relationship between temperature and the occurrence of zeolite minerals. For example, higher temperature favors mordenite over heulandite (Hawkins *et al.,* 1978; Bish *et al.,* 1982; Kitsopoulos, 1997).

K-rich feldspar, which is probably authigenic, displays a polygonal grain boundary at the margin of heulandite veins. This observation suggests textural equilibrium and indicates that K-rich feldspar crystallized with heulandite.

Because precursor minerals contain only trace K levels, the source of K for illitization must be predominantly controlled by fluid chemistry and, to a lesser degree, by precursor minerals. At high fluid/rock ratios, smectite seems to occur in the early stage of alteration. In contrast, zeolite minerals and authigenic K-rich feldspar progressively occurred later as the fluid/rock ratio decreased.

### *Implications for fault activity*

K-Ar data on clay minerals have proved extremely useful in understanding the historical aspects of diagenetic change from smectite to illite and I-S interstratification (Clauer and Chaudhuri, 1996; Velde and Renac, 1996; Clauer *et al.,* 1997). The absolute age of final movement along faults may be determined also by applying K-Ar techniques to the illitic fraction of fault gouges. Lyons and Snellenburg (1971) applied K-Ar techniques to illitic materials as a method to determine the ages of the last movement along fault planes. Although fault-gouge illite may be contaminated by admixtures of detrital illite and micas, illite from fault gouges has been shown to yield an absolute age in close agreement with geologically inferred dates of the termination of faulting (Lyons and Snellenburg, 1971; Kralik *et al.,* 1987; Tanaka *et al.,* 1995).

The K-Ar ages of illite or I-S minerals of gouges may be influenced by several factors (Velde and Renac, 1996), including clay diagenesis and the recycling of K of the clay fraction, and dissolution of detrital mica clays by weathering, coupled with the influx of additional K from outside the fault system. However, in this study there is no evidence from SEM or XRD that neither neoformation of the clays in gouges nor contamination from parent rocks occurred. On the basis of our results, illite probably formed by dissolution/precipitation processes. Tanaka *et al.* (1995) showed that the clay minerals present in the $<1$-μm size fraction of fault gouges are mostly formed by neoformation processes resulting from hydrothermal alteration. Our study shows evidence of neoformation of illitic clays in the fault gouges. Thus, the K-Ar system may have been reset during hydrothermal alteration. Accordingly, the K-Ar ages of the fault gouges containing K are probably the age of the hydrothermal events associated with the movement of the Dongrae fault.

Although there is no direct evidence that the fault-gouge materials are genetically related to the hydrothermal-alteration processes, we may suggest a history for the formation of fault-gouge materials, both from the above data and from data relating to the larger Yangsan fault system. Most granite bodies of the Bulguksa intrusive rocks are closely related by spatial distribution along the Yangsan fault system, and thus a genetic relationship may exist between the fault and intrusive events. Granitic rocks distributed near the Yangsan fault system yield ages ranging from 90 to 62 Ma by K-Ar and Rb-Sr dating methods (Lee, 1976; Min *et al.,* 1982; Lee *et al.,* 1995). Granite intrusions may have regulated fault activity on the basis that the intrusion events predated faulting activity. Sedimentary rocks near the Yangsan fault are of apparent ages of 93.4 ± 2.5 Ma by K-Ar dating methods (Chang and Choo, 1998). Because these sedimentary rocks commonly contain detrital K-rich micas or diagenetic clay minerals, the apparent ages differ from those obtained from the secondary minerals of the gouges in the Dongrae fault. On the basis of results presented here, it is unclear if the K-Ar ages indicate the beginning of the movement of this fault. Nonetheless, all age dates obtained here indicate that the Dongrae fault was most active in the Eocene. Hydrothermal fluids associated with granitic rocks probably circulated throughout the fracture zones. Consequently, secondary minerals in the gouges were the result of direct precipitation between the hydrothermal solutions and pulverized materials. Therefore, clay minerals, zeolite, K-rich feldspar, apatite, and pyrite may be the product of the hydrothermal activity related to fault activity.

From an analysis of paleostress of the Yangsan fault (Chang and Chang, 1998; Cho and Chang, 1998), the Yangsan fault system has undergone multiple deformation activity involving complex fault movements

consisting of strike-slip and dip-slip components in the early Eocene. Such a complex faulting mechanism may involve fluid-assisted deformation along the gouge zone. The high porosity and permeability of pulverized materials may facilitate an influx of hydrothermal fluid which subsequently reacts with gouge materials to form clay minerals. However, not all of the clast materials in the fault-fracture zones may produce clay minerals without additional fluids. Fracturing and hydrothermal alteration may repeatedly occur with elevated fluid pressure induced by the reduction of pore volume when clay minerals and other secondary minerals form (Chang and Choo, 1998).

The small number of K-Ar dates obtained here is not sufficient to provide genetic information on the fault motion of the Dongrae fault. Mineralogical and isotopic methods are required on many more gouge materials to establish the age of the fault activity.

## ACKNOWLEDGMENTS

The authors thank S. Guggenheim, W.D. Huff, J.L. Cronson, and T.J. Algeo for their helpful suggestions and reviews of the manuscript. This study was partly supported by a research grant from Korea Science and Engineering Foundation (96-0703-05-01-3).

## REFERENCES

Baxter Grubb, S.M., Peacor, D.R., and Jiang, W.T. (1991) Transmission electron microscope observations of illite polytypism. *Clays and Clay Minerals,* **39,** 540–550.

Bish, D.L., Vaniman, D.T., Byers, F.M., and Broxton, D.E. (1982) *Summary of the Mineralogy-Petrology of Tuffs from Yucca Mountain and the Secondary-Phase Thermal Stability in Tuffs.* Los Alamos National Laboratory Report LA-9321-MS, 47pp.

Caine, J.S., Evans, J.P., and Forster, C.B. (1996) Fault zone architecture and permeability structure. *Geology,* **24,** 1025–1028.

Chang, C.J. and Chang, T.W. (1998) Movement history of the Yangsan Fault based on paleostress analysis. *Journal of Engineering Geology of Korea,* **8,** 35–50.

Chang, T.W. and Choo, C.O. (1998) Faulting processes and K-Ar ages of fault gouges in the Yangsan Fault Zone. *Journal of Earth Science of Korea,* **20,** 25–37.

Chester, F.M. and Logan, J.M. (1987) Composite planar fabric of gouge from the Punchbowl Fault, California. *Journal of Structural Geology,* **9,** 621–634.

Chester, F.M., Evans, J.P., and Biegel, R.L. (1993) Internal structure and weakening mechanisms of the San Andreas Fault. *Journal of Geophysical Research,* **98,** 771–786.

Cho, Y.C. and Chang, T.W. (1998) Analysis of paleostress of the Dongrae Fault. *The Economic and Environmental Geology of Korea, Annual Conference Abstract,* 109.

Choo, C.O. (1996) Mineralogy and genesis of Napseok (sericite, pyrophyllite, dickite) in the Kimhae area, Korea. Ph.D. dissertation, Seoul National University, Seoul, Korea, 190 pp.

Clauer, N. and Chaudhuri, S. (1996) Inter-basinal comparison of the diagenetic evolution of illite/smectite minerals in buried shales on the basis of K-Ar systematics. *Clays and Clay Minerals,* **44,** 818–824.

Clauer, N., Środoń, J., Francu, J., and Sucha, V. (1997) K-Ar dating of illite fundamental particles separated from illite-smectite. *Clay Minerals,* **32,** 181–196.

Hawkins, D.B., Sheppard, R.A., and Gude, A.J., 3rd (1978) Hydrothermal systhesis of clinoptilolite and comments on the assemblage phillipsite-mordenite. In *Natural Zeolites: Occurrence, Properties, Use,* L.B. Sand and F.A. Mumpton, eds., Pergamon Press, Elmsford, New York, 337–343.

Inoue, A., Velde, B., Meunier, A., and Touchard, G. (1988) Mechanism of illite transformation during smectite-to-illite conversion in a hydrothermal system. *American Mineralogist,* **73,** 1325–1334.

Kerrisk, J.F. (1983) *Reaction-Path Calculations of Groundwater Chemistry and Mineral Formation at Rainier Mesa, Nevada.* Los Alamos National Laboratory Report LA-9912-MS, 41 pp.

Kim, I.S. and Kim, J.Y. (1983) Electric resistivity survey in Eonyang Fault area, southeastern Korean peninsula. *Journal of Mining Geology of Korea,* **16,** 11–18.

Kim, O.J. (1987) Tectonic evolution. In *Geology of Korea,* D.S. Lee, ed., Kyogak-Sa Publishing Company, Seoul, 253–263.

Kim, Y.H. and Lee, K. (1988) A geoelectric study on the structure of the Yangsan Fault in the south of Kyeongju. *Journal of Geological Society of Korea,* **24,** 47–61.

Kitsopoulos, K.P. (1997) The genesis of a mordenite deposit by hydrothermal alteration of pyroclastics on Polyegos Island, Greece. *Clays and Clay Minerals,* **45,** 632–648.

Kralik, M., Klima, K., and Riedmüller, G. (1987) Dating fault gouges. *Nature,* **327,** 315–317.

Lee, J.I., Kagami, H., and Nagao, K. (1995) Rb-Sr and K-Ar age determinations of the granitic rocks in the southern part of the Kyeongsang basin, Korea: Implication for cooling history and evolution of granitic magmatism during late Cretaceous. *Geochemistry Journal,* **29,** 363–376.

Lee, K. and Jin, Y.G. (1991) Segmentation of the Yangsan Fault System: Geophysical studies on major faults in the Kyeongsang basin. *Journal of Geological Society of Korea,* **27,** 434–449.

Lee, K. and Na, S.H. (1983) A study of microearthquake activity along the Yangsan Fault. *Journal of Geological Society of Korea,* **19,** 127–135.

Lee, K., Cheon, K., and Um, C.R. (1992) Geoelectric surveys of the Dongrae Fault, the Eonyang Fault and the Ilkwang Fault: Geophysical studies on major faults in the Kyeongsang basin. *Journal of Geological Society of Korea,* **28,** 218–226.

Lee, Y.J. (1976) K-Ar ages of granitic rocks in Eonyang and northwestern Ulsan areas, Korea. *Journal of Mining Geology of Korea,* **9,** 127–134.

Lyons, J.B. and Snellenburg, J. (1971) Dating faults. *Geological Society of America Bulletin,* **82,** 1749–1752.

Min, K.D., Kim, O.J., Yun, S., Lee, D.S., and Joo, S.H. (1982) An applicability of plate tectonics to the post-Late Cretaceous igneous activities and mineralization in the southern part of south Korea (I). *Journal of Mining Geology of Korea,* **15,** 123–154.

Morrow, C.A., Shi, L.Q., and Byerlee, J.D. (1984) Permeability of fault gouge under confining pressure and shear stress. *Journal of Geophysical Research,* **89,** 3193–3200.

Shibata, K. and Tagaki, H. (1988) Isotopic ages of rocks and intrafault materials along the Median Tectonic Line—An example in the Bungui-toge area, Nagano Prefecture. *Journal of Geological Society of Japan,* **94,** 35–50.

Shimazaki, H. and Lee, M.S. (1981) Reconnaissance on I- and S- type granitoids in southern Korea. *Journal of Geological Society of Korea,* **17,** 189–193.

Tagaki, H. and Kobayashi, K. (1996) Composite planar fabrics of fault gouges and mylonite-compositive petrofabrics. *Journal of Geological Society of Japan,* **102,** 170–179.

Tagaki, H., Shibata, K., Sugiyama, Y., Uchiumi, S., and Matsumoto, A. (1989) Isotopic ages of rocks along the Median

Tectonic Line in the Kayumi area, Mie Prefecture. *Journal of Mineralogy, Petrology and Economic Geology,* **84,** 75–88.

Tanaka, H., Uehara, N., and Itaya, T. (1995) Timing of the cataclastic deformation along the Akahashi Tectonic Line, central Japan. *Contributions to Mineralogy and Petrology,* **120,** 150–158.

Velde, B. and Renac, C. (1996) Smectite to illite conversion and K-Ar ages. *Clay Minerals,* **31,** 25–32.

Yau, Y.C., Peacor, D.R., and Essene, E.J. (1987) Hydrothermal treatment of smectite, illite, and basalt to 460 °C: Comparison of natural with hydrothermally formed clay minerals. *Clays and Clay Minerals,* **35,** 241–250.

E-mail of corresponding author: chooco@kis.kigam.re.kr

*(Received 2 November 1998; accepted 20 November 1999; Ms. 98-130; A.E. Warren D. Huff)*